Materials and Structures
DOI 10.1617/s11527-011-9777-y

ORIGINAL ARTICLE

A nonlinear constitutive relationship for asphalt binders

Rodrigo Delgadillo · Hussain U. Bahia · Rod Lakes

Received: 7 June 2010 / Accepted: 29 August 2011

Abstract A nonlinear constitutive relationship was developed for asphalt binders. Two binders, one polymer modified and one unmodified, were tested in shear using creep and recovery loading. Five different stress levels and four loading times were considered, to capture the response of the binders in the linear and nonlinear viscoelastic range. The creep response of the binders was successfully modeled with a nonlinear power law function. The modified superposition principle was unable to predict the recovery phase of the testing data. A nonlinear constitutive relationship composed of a nonlinear viscous part plus a linear viscoelastic part was developed. The constitutive relationships successfully predicted the binders' response in creep and recovery. The predictions of the constitutive relationships matched accurately the response of the binders subjected to the Multiple Stress Creep and Recovery loading pattern.

Keywords Asphalt · Asphalt cement · Asphalt binder · Viscoelasticity · Nonlinearity · Nonlinear viscoelasticity · Constitutive relationship

R. Delgadillo (✉)
Department of Civil Engineering, Universidad Técnica Federico Santa Maria, Av. España 1680, Valparaiso, Chile
e-mail: rodrigo.delgadillo@usm.cl

H. U. Bahia
Department of Civil and Environmental Engineering, The University of Wisconsin—Madison, 3350 Engineering Hall, 1415 Engineering Dr., Madison, WI 53706, USA
e-mail: bahia@engr.wisc.edu

R. Lakes
Department of Engineering Physics, The University of Wisconsin—Madison, 541 Engineering Research Building, 1500 Engineering Dr., Madison, WI 53706, USA
e-mail: lakes@engr.wisc.edu

Published online: 10 September 2011

1 Introduction

Asphalt binders are one of the load carrying components of asphalt mixtures for pavements. They are obtained from the refining of crude oil. They are produced from the heavy residue after the distillation of fuels and lubricants. Asphalt binders are viscoelastic materials. Their response is time and temperature dependent [1, 7, 16]. With higher temperatures and longer loading times, the asphalt becomes softer and behaves more like a viscous fluid. With lower temperatures and fast loads, the asphalt becomes stiffer and more elastic.

Viscoelastic materials can be linear or nonlinear. In linear materials, for a specific temperature and point in time, the strain is proportional to the stress. This does not hold true for nonlinear materials [20]. Asphalt binders behave as linear viscoelastic materials for low stress levels and as nonlinear viscoelastic high stresses. The threshold for the linear region depends on the composition of asphalt binder, the loading time, and the temperature [11].

Because of the random distribution of the particles inside the asphalt mixture, there are important variations in the internal stresses (strains) when the mixture is loaded [21]. Specifically in the binder, the variations can be significant. Previous research has shown that the binder strains can vary between 1 and 500 times the mixture strain [17, 18]. For these reasons, when the asphalt mixture is subjected to traffic loading, some of the binder performs in the linear viscoelastic region and some of the binder reaches the region of nonlinear behavior.

Characterizing asphalt binders in the linear and nonlinear range is critical for proper material selection for asphalt pavements. The response of the material has to be known for the range of stresses and loading times expected when used inside the pavement. Nowadays, however, the asphalt characterization is based on testing carried out with very low stresses and short times, in the linear viscoelastic region. Two binders that have similar characteristics in the linear region do not necessarily behave in a similar way in the nonlinear region [11]. A characterization of the asphalt binders that includes the nonlinear region is needed.

In the present work, a nonlinear constitutive relationship was formulated and validated for two asphalt binders: one plastomer polymer modified (Elvaloy®, 2% by weight) and one unmodified. The binders were tested with creep and recovery loading at different times and stresses, using a dynamic shear rheometer (DSR) with cone and plate geometry. The work is part of a more comprehensive research effort that studied the relationship between binder nonlinear response and mixture rutting [9]. The temperatures relevant for asphalt mixture rutting are the high pavement temperatures. For this reason, the temperature considered for the testing was equal to 46°C, which is in the high temperature range for pavements.

2 Background

2.1 Linear viscoelasticity

Figure 1 shows the schematics for the creep response of a viscoelastic material. The strain response $\gamma(t)$ presents an instantaneous deformation as soon as the stress τ_0 is applied at time 0. Then an increase in $\gamma(t)$ is observed, as τ_0 is kept constant between 0 and t_1. After τ_0 is removed, the material shows a recovery in the deformation, which can be partial or total.

The ratio between $\gamma(t)$ and τ_0 is called creep compliance $J(t)$. If the $J(t)$ function is independent of the stress level, the material is considered linear viscoelastic.

$$J(t) = \frac{\gamma(t)}{\tau_0} \tag{1}$$

where τ_0 is the stress applied, t_1 is the loading time, γ is the total strain after loading phase, γ_r is the recoverable strain, measured after full recovery is achieved (long enough resting time), γ_p is the permanent strain, measured after full recovery is achieved (long enough resting time).

In a linear viscoelastic material, the effect of combined load is equal to the sum of the effects of the individual loads. This is known as the Boltzmann superposition principle [4]. Using this principle, constitutive relations can be obtained for linearly viscoelastic materials, which describe the response of the material due to an arbitrary load history. Equation 2 is known as the Boltzmann superposition integral for strain, and it represents the creep response of a linear viscoelastic material subjected to an arbitrary stress history $\tau(\xi)$, where ξ is the time integration variable, and stress starts at $t = 0$.

$$\gamma(t) = \int_0^t J(t-\xi)\frac{\mathrm{d}\tau(\xi)}{\mathrm{d}\xi}\mathrm{d}\xi \tag{2}$$

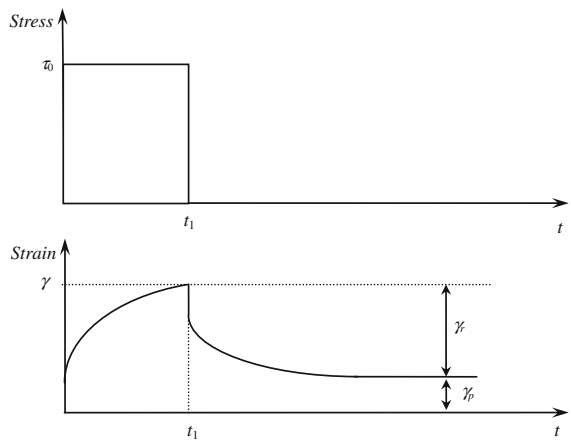

Fig. 1 Creep-recovery loading and strain response of a viscoelastic material

Both the Riemann integral form and the Stieltjes integral form could be used with step stress histories. When the Riemann form is selected, as in this paper, the Heaviside step function is used to mathematically represent the step stresses.

2.2 Nonlinear viscoelasticity

For some viscoelastic materials the viscoelastic functions depended on the stress or strain level, and the material is called nonlinear viscoelastic. Superposition is not valid for nonlinear materials, and obtaining the constitutive relations becomes more complex. Multiple integral relations are one option, but significant numbers of tests are usually required to determine the kernel functions [22]. The nonlinearity can also be incorporated into a single integral with a nonlinear integrand, using a modified superposition principle. This approximation is not as flexible as the multiple integral representations, but it is accurate enough for many practical purposes [14]. If several mathematical conditions need to be satisfied [25], and the creep compliance is allowed to depend on both time and stress, a constitutive relation can be obtained for the nonlinear material with the following form [14]:

$$\gamma(t) = \int_0^t J(t-\xi,\tau)\frac{\mathrm{d}\tau(\xi)}{\mathrm{d}\xi}\mathrm{d}\xi \tag{3}$$

where $\gamma(t)$ is the nonlinear strain response, $J(t,\tau)$ is the creep compliance as a function of stress and time, τ is the stress history function, and ξ is the time integration variable. There are other interpretations for the stress to be considered inside the compliance function during the unloading phase. Ward et al. [31] assumed the compliance after t_1 to be a result of the change in stress. Sternstein [29] considered the compliance after time t_1 as a result of the final stress.

Other approaches for characterizing nonlinear viscoelastic materials have been developed by combining viscoelastic and viscoplastic elements [19, 27, 28]. In nonlinearly viscoelastic materials, recovery need not follow the same time dependence as creep. Such behavior has proven difficult to model in polymers using nonlinear superposition. The Schapery model can provide more flexibility in such cases at the expense of greater complexity in a single integral model [5].

2.3 State of the art in nonlinear characterization of asphalt binders

The current Superpave specifications for asphalt binders include a procedure for accounting for high traffic loads. The procedure is very simplistic and consists basically of using a stiffer binder than the one normally needed. However, since the binder characterization is carried out using only low stress levels, this only ensures that the binder is stiffer in the low stress range.

An improvement in the characterization of asphalt binders constitute the dual parameter proposed by Reinke et al. [26]. They propose to measure the complex viscosity η^* of the binder in the linear viscoelastic region and also the stress level where η^* decreases to 70% of its initial value. By measuring the stress range where the complex viscosity does not degrade considerably, the contribution of the binder to permanent deformation is characterized in a more rational way. Their parameter is called Stress Viscosity Factor, and it is equal to the multiplication between η^* and the stress level where η^* decreases to 70%.

The Expert Task Group of the Federal Highway Administration (FHWA) has recently approved a protocol to evaluate the stress sensitivity of asphalt binders using the DSR called multiple stress creep and recovery (MSCR). The MSCR protocol is run using a constant stress creep of 1 s duration followed by a zero stress recovery of 9 s. The test is run at two stress levels: 0.1 and 3.2 kPa. Ten cycles are run at each of the two stress levels for a total of 20 cycles. There are no rest periods between creep and recovery cycles or changes in stress level. The full details of the testing protocol are described in the ASTM D7405-10a standard. For each stress level, a parameter called nonrecoverable compliance J_{nr} is calculated. J_{nr} for 0.1 kPa is equal to the strain after the 10 cycles run at that stress level, divided by that stress. The definition for J_{nr} at 3.2 kPa is analogous [8].

The J_{nr} parameter has been suggested as a measure of the binder contribution to mixture permanent deformation. The parameter has, however, several limitations, since the conditions used in the testing are arbitrary. The two selected stress levels are arbitrary and do not necessarily represent the stresses of the binder inside the pavement. The number of cycles and time of loading do not cover a wide span,

which is necessary to characterize long term permanent deformation in the material. The recovery time allowed in the test is not long enough, modified binders are still recovering after the 9 s of unloading phase [12].

Mechanical analogs have been used by some authors [13, 23]. These approaches provide intuitive models that can be somehow related to the physical nature of materials. They, however, lack the flexibility needed to model complex material responses. Also, the separation between non-linear and linear elements is not easy to define objectively.

In the present work, a nonlinear viscoelastic constitutive relationship was developed, for modeling the response of binders in a wide range of times and stresses. A nonlinear constitutive relation allows for modeling the response of the binder for a wide range of times and stresses, in the linear and nonlinear viscoelastic range. A constitutive relationship for asphalt binders in the nonlinear range, like the one presented in this paper, has not been previously obtained. Nor has been defined which of the nonlinear modeling approaches is the most convenient for this type of materials.

3 Binder testing

3.1 Test description

A DSR, make Paar Physica, model SmartPave was used for the binder testing. Cone and plate geometry was selected, to ensure homogeneous shear rate throughout the sample, which is essential for nonlinear characterization. The cone and plate characteristics are 25 mm diameter, 49 μm gap (distance between tip of cone and plate), and 1° of cone angle.

Two different binders were selected for testing. The first one is an unmodified binder labeled N3, with a performance grade PG70-22. The second binder was modified with a plastomer polymer called Elvaloy®. The binder was labeled as B5, and it had a performance grade PG64-34. These two binders were selected with the objective of comparing the benefits of a more elastic but softer binder, like the polymer modified one, versus a stiffer but less elastic binder, like the unmodified one. Previous research has shown that the permanent strain of softer more elastic binders can be lower than the permanent strain of harder less elastic binders, when subjected to stresses in the linear viscoelastic range [12]. It is also known that the stress dependency of polymer modified binders is different from unmodified binders [3, 11]. So comparison of both types of binders at high stress levels is also of interest. The two binders selected are commonly used in the asphalt paving industry.

Traffic loads on pavement are characterized by a loading pulse (the tire load) followed by a resting time (time in between vehicles) [15]. For this reason, creep and recovery testing was selected as the type of testing that better represented the asphalt binder loading conditions on service. The schematics of the loading and response were shown in Fig. 1.

For a nonlinear viscoelastic material, γ depends on the loading time and on the testing stress. The same applies to γ_r and γ_p.

$$\gamma_r = \gamma_r(\tau_0, t_1);\ \gamma_p = \gamma_p(\tau_0, t_1);\ \gamma = \gamma_r + \gamma_p = \gamma(\tau_0, t_1) \tag{4}$$

In order to capture the nonlinear viscoelastic behavior of the asphalt binders, the variables that needed to be varied during the testing were loading time and applied stress. The variations of the nonlinear binder properties with temperature were out of the scope of this study. Only one temperature was selected for the binder testing. This temperature was 46°C, which is approximately the average pavement temperature during the summer in Wisconsin.

The shear stress was varied between a minimum value of 0.1 kPa and a maximum value of 30 kPa. The minimum value was selected in order to ensure that the binders would behave linearly at 46°C. Previous research [11] showed linear viscoelastic behavior of similar asphalt binders at 46°C and 0.1 kPa. The maximum stress level considered corresponded to the maximum torque capacity of the testing device. Previous work demonstrated that at 46°C high nonlinearity is expected in asphalt binders subjected to 30 kPa of shear stress [11]. By varying the stresses between these two values, the properties of the binder in the linear viscoelastic range and in the nonlinear viscoelastic range were expected to be captured.

The loading time was varied between 1 and 1,000 s, at tenfold increments. The minimum loading

Table 1 Testing plan for asphalt binders

Binder type	Stress level (kPa)	Creep/recovery time (s)			
Unmodified (PG70-22)	0.1	1/2000	10/10000	100/20000	1000/40000
	1	1/2000	10/10000	100/20000	1000/40000
	10	1/2000	10/10000	100/20000	1000/40000
	20	1/2000	10/10000	100/20000	1000/40000
	30	1/2000	10/10000	100/20000	1000/40000

time of 1 s is much bigger than the rise time of the machine, which is on the order of 10^{-4} s, which ensured accuracy of the measured values. No experiment can provide a true instantaneous deformation. At the temperature used, the time scale of the creep protocol was not short enough to probe the glassy regime.

In order to determine the non recoverable strain γ_p, enough recovery time needs to be allowed in the samples. It is common to consider a ratio between the loading time and the recovery time of 1/10. However, previous research has shown that such a ratio is not enough to allow full recovery of asphalt binders [12]. This is especially critical in the case of polymer modified binders, which usually show high levels of delayed elasticity. In the present work, extremely long recovery times were considered, in order to allow full recovery of the binders. These recovery times are in no way practical or suitable to be implemented in more standardized testing. However, the results of the testing are expected to suggest practical ranges for the recovery phase. In other words, the results of the test will allow determining the times after which the recovery is not significant anymore. In this way, shorter recovery times might be recommended for future testing. The binder testing program is presented in Table 1 for the unmodified binder. The testing program for the polymer modified binder is exactly the same.

The binders were subjected to primary aging, using a Rotational Thin Film Oven (AASHTO T-240) before being tested, to represent the state of the binder in service right after construction.

3.2 Test results

3.2.1 Polymer modified binder

The results from the polymer modified binder testing indicated a power law behavior for short loading times. Figure 2 shows the shear strains for 1 s loading time in a log–log scale. The strain used is the engineering strain. The response will probably look different if another strain is selected, like true strain for example. The engineering strain was selected between all the Seth–Hill strain families because it is the most relevant to the field of application of the work. The response that needs to be quantified is the deformation of the material with respect to its original dimensions.

For all stress levels, the loading phase could be approximated by a straight line. For longer loading times, the power law behavior was still observed for 0.1 and 1 kPa. At the higher stress levels, however, two different slopes were observed for the shear strain, as shown in Fig. 3. It can be observed that the point in time where the change in slope occurs decreased when the stress was increased.

High recovery was observed after the load was removed. The recovery continued for very long times. Figure 2 shows that for 1 s of loading, the recovery of the binders is far from complete after 10 s of resting time. Only after 100 s of resting time, 90% or more of the recovery was achieved for all stress levels. After 1,000 s of resting time, at least 98% of the recovery was obtained in all cases. The apparent increase in strain for longer times for 0.1 and 1 kPa is due to the precision of the testing machine and it is not significant.

In order to verify the nonlinear response of the polymer modified binder, the creep compliance of the loading phase was plotted in log–log scale. The results are presented in Fig. 4 for the five stress levels used and 1,000 s of loading time. A linear behavior was observed for 0.1 and 1 kPa for the whole time range considered, suggesting a power law behavior. For 10, 20 and 30 kPa, linear behavior was observed for shorter times. Nonlinear behavior was observed for longer times for these stress levels. The point in time for the transition between linear viscoelastic and nonlinear viscoelastic behavior decreased when the

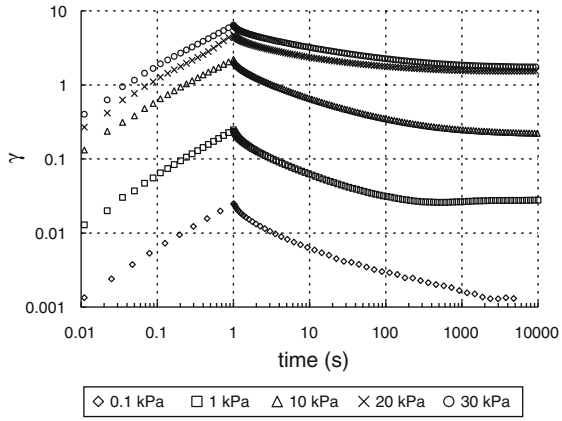

Fig. 2 Creep and recovery test results, polymer modified binder, 1 s loading time, 5 stress levels

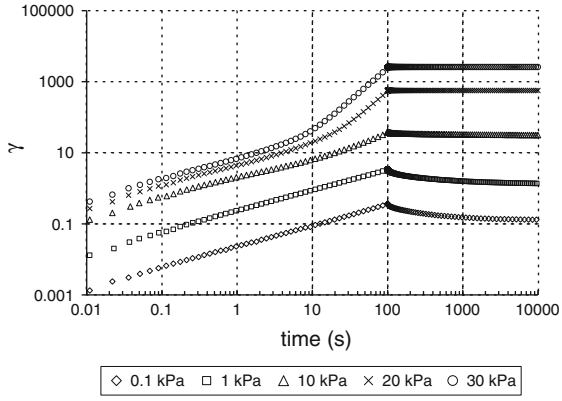

Fig. 3 Creep and recovery test results, polymer modified binder, 100 s loading time, 5 stress levels

stress was increased. The samples tested at 20 and 30 kPa failed after 440 and 580 s of loading, respectively, which is why the plots for these stresses do not reach 1,000 s. The failure of samples in the DSR at the testing temperature happens because of edge effects that modify the geometry of the original sample [2].

3.2.2 Unmodified binder

The unmodified binder showed a power law behavior for most of the time range considered during the test. A straight line with a single slope characterized the loading phase during the whole time range for 0.1 and 1 kPa. For the other three stress levels (10, 20 and 30 kPa), a small increase in the slope of deformation was observed but for longer time periods. This steepening of the slope was much smaller than that

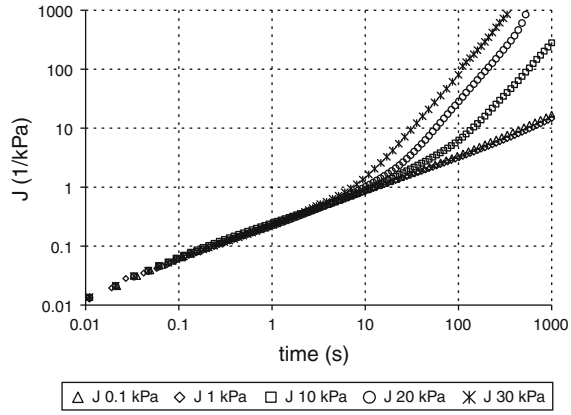

Fig. 4 Creep compliance loading phase, polymer modified binder, 1,000 s loading time

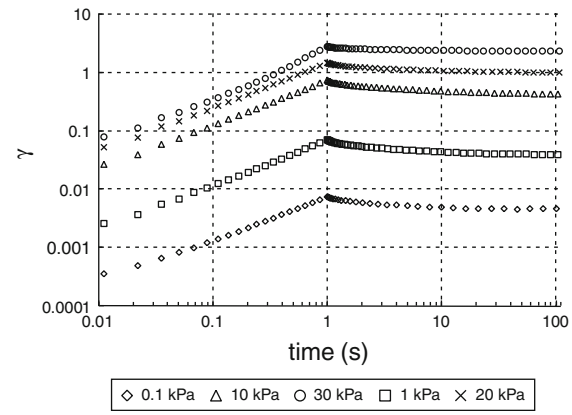

Fig. 5 Creep and recovery test results, unmodified binder, 1 s loading time

observed for the modified binder. Figures 5 and 6 present the creep and recovery test results for 1 s of loading time and 1,000 s of loading time, respectively.

The recovery of the binder after removing the load was not as important as in the modified binder. Also, the time required for full recovery was much shorter than the one observed for the modified binder. The usual ratio of 1/10 between loading time and unloading time was enough to achieve most of the recovery in all cases except for 1 s loading time, where a ratio of 1/20 seemed to be better suited. For 1,000 s of loading time, an unloading time of 1,000 s was enough to achieve most of the recovery.

The creep compliance of the loading phase was plotted in a log–log scale in order to check the linearity of the response for the unmodified binder.

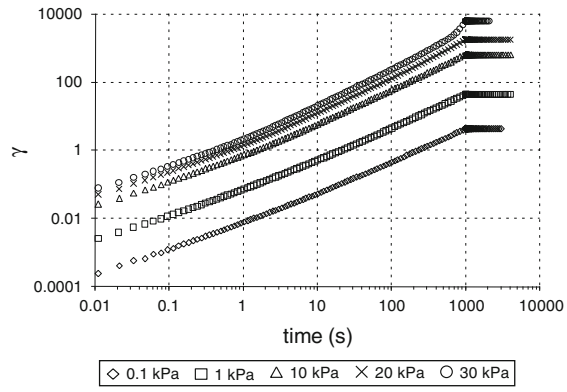

Fig. 6 Creep and recovery test results, unmodified binder, 1,000 s loading time

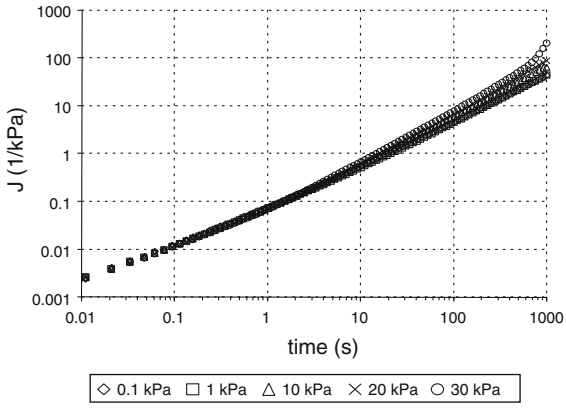

Fig. 7 Creep compliance loading phase, unmodified binder, 1,000 s loading time

Figure 7 shows the results for the five stress levels and 1,000 s of loading time. A linear behavior was observed for 0.1 and 1 kPa for the whole time range considered, suggesting a power law behavior. For 10, 20 and 30 kPa, linear behavior was observed for shorter times, below 1 s. After that, nonlinear behavior was observed. The nonlinearity observed for the unmodified binder was, however, less significant than for the modified binder.

4 Characterization of the loading phase

4.1 Polymer modified binder

Considering the shape of the curves in the log–log scale, nonlinear power representation was selected to model the material's response during the loading phase. The nonlinear power representation is given by the following equation:

$$\gamma(t,\tau) = \sum_{i=1}^{n} k_i \cdot t^{m_i} \cdot \tau^{p_i} \tag{5}$$

where γ is the shear strain (dimensionless), t is the time (s), τ is the shear stress (kPa), k_i, m_i, p_i are the model parameters

The time t in Eq. 5 and in subsequent equations based on it, is given by $t = t(\text{s})/t_{\text{std}}$ in which $t_{\text{std}} = 1$ s. The stress τ is given by $\tau = \tau(\text{kPa})/\tau_{\text{std}}$ in which $\tau_{\text{std}} = 1$ kPa. The letters *std* are used as a subscript to indicate standard value. The model parameter k_i is dimensionless. The units for equations based on Eq. 5 are referred to the above clarification. The number of arguments n to be used depends on the material. For the polymer modified binder, a value of n equal to two was found to be enough to describe the shape of the curves. This is logical considering that the curves show a linear shape with two different slopes. These types of equations are also known as Nutting's type equations [24]. The material constants k_i in these equations have no physical meaning [6].

Nonlinear curve fitting was used to determine the parameters of the model, with the aid of Kaleida-Graph® software [30]. The fitting parameters were estimated using the binder strain data of the loading phase for all the testing stresses together. In order to give the same importance to the low strain/time range and the high strain/time range, the fitting was weighed using the strain as the weighing variable. The fitting showed to be very good, with an R^2 value of 0.996. The results of the fitting are presented in Eq. 6.

$$\gamma(t,\tau) = 0.227 \cdot t^{0.587} \cdot \tau^{0.994} + 2.28 \times 10^{-7} \cdot t^{2.00} \cdot \tau^{4.03} \tag{6}$$

where γ is dimensionless, and the units of t and τ are as defined previously. The first argument in the equation represents the behavior at low stress levels and shorter times. The power parameter for the stress variable τ is almost equal to one, which confirms the linear dependency of strain on stress level in the short times—low stress region. The second argument in the equation represents the nonlinear behavior at higher stresses and longer loading times. As it can be seen, the power for the stress parameter is much higher than one, which indicates high nonlinearity.

To allow simplification of the model, a second fitting was carried out with the assumption of linearity (power of one for the stress variable) in the first argument. Equation 7 shows the results of the fitting. The goodness of the fitting was not significantly altered ($R^2 = 0.995$), and also the other constants did not change significantly.

$$\gamma(t,\tau) = 0.226 \cdot t^{0.589} \cdot \tau + 2.06 \times 10^{-7} \cdot t^{2.04} \cdot \tau^{4.04} \quad (7)$$

The units of Eq. 7 are as defined for Eq. 6. Figure 8 shows the creep data and the fitting using Eq. 7. Dependence on both time and stress variables is shown in Fig. 9 as a three dimensional plot.

The creep compliance of the material J is obtained by dividing the shear strain by the shear stress. The compliance is a nonlinear function of loading time (t) and stress level (τ), as shown in Eq. 8.

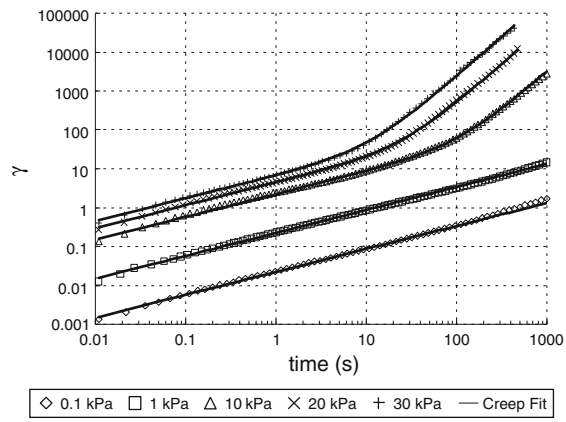

Fig. 8 Creep fit polymer modified binder

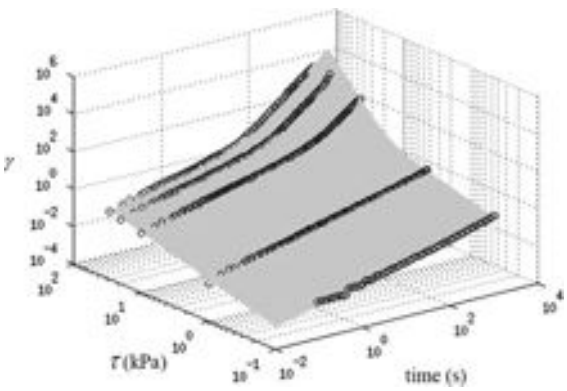

Fig. 9 Creep fit polymer modified binder—3D

$$J(t,\tau) = 0.226 \cdot t^{0.589} + 2.06 \times 10^{-7} \cdot t^{2.04} \cdot \tau^{3.04}\ (1/\text{kPa}) \quad (8)$$

4.2 Unmodified binder

The shape of the creep curves measured for the unmodified binder also suggested the use of the nonlinear power law. Again, two arguments in the model were enough to describe the material behavior in creep loading. Two different fittings were tried: in the first one the p_1 parameter (power of stress variable τ) from Eq. 5 was allowed to vary freely; in the second fit the p_1 value was fixed at one. The goodness of fitting for both cases was found to be very good, as the R^2 values calculated were 0.993 for the first model and 0.990 for the second one. The second model was selected because of the simplifications allowed by the linearity in the first argument. Equation 9 shows the creep fitting function for the unmodified binder:

$$\gamma(t,\tau) = 7.11 \times 10^{-2} \cdot t^{0.807} \cdot \tau + 3.37 \times 10^{-3} \cdot t^{1.34} \cdot \tau^{1.25} \quad (9)$$

The creep data and fitting using Eq. 10 are shown in Fig. 10.

In Eq. 9, the nonlinearity of the second term, as shown by the power of the stress variable τ, is not as high as it was for the polymer modified binder discussed in the previous section. The creep compliance for the unmodified binder, obtained by dividing Eq. 9 by the stress, is given by Eq. 10.

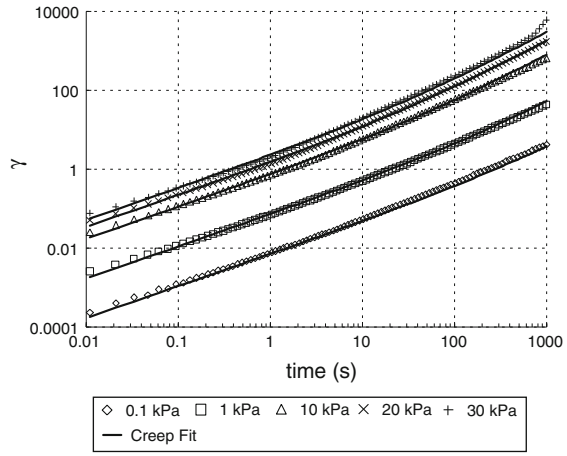

Fig. 10 Creep fit unmodified binder

$$J(t,\tau) = 7.11 \times 10^{-2} \cdot t^{0.807} + 3.37 \times 10^{-3} \cdot t^{1.34} \cdot \tau^{0.25} \quad (1/\text{kPa}) \tag{10}$$

The model is empirical. The underlying physical mechanisms of asphalt as a complex material are not addressed here. Equations 8 and 10 do not comply with the fading memory hypothesis, which means that superposition cannot be directly applied, as it will be shown later in this paper. Also, they do not comply with the invariance requirements from the continuum mechanics standpoint, so they cannot be extended to represent the creep behavior under multiple stress states. As with other models for nonlinear behavior of polymers it is difficult to handle recovery. The equations, however, do successfully model nonlinear creep and recovery response for all stress levels at different loading times. The models were also found to correlate satisfactorily with the permanent deformation of asphalt mixtures containing the same binders tested here, as it is shown in another work [10].

5 Constitutive relationships

5.1 Prediction of recovery using modified superposition principle

The first attempt to characterize the nonlinear behavior of the binder's recovery phase was based on the direct application of the modified superposition principle. Following this principle, the effect of the loading and unloading (creep and recovery) would be equal to the effect of applying a constant stress at time zero, plus the effect of applying an equivalent but negative stress at the time the load is supposed to be removed. Three different interpretations for the stress to be used in the creep compliance function during the recovery phase were discussed previously. When the recovery stress is equal to zero, as in the creep and recovery test performed, the three interpretations are reduced to only two different equations. The resulting two equations for the recovery phase ($t > t_1$), expressed in shear form, are as follows:

$$\gamma(t) = \tau_0 J(t,\tau_0) - \tau_0 J(t-t_1,\tau_0) \tag{11}$$

$$\gamma(t) = \tau_0 J(t,\tau_0) - \tau_0 J(t-t_1,0) \tag{12}$$

where J is the nonlinear creep compliance, τ_0 is the constant shear stress applied during the loading phase, and t_1 is the loading time.

For the polymer modified binder, the creep compliance J of the loading phase was described previously using Eq. 8. By substituting J from Eq. 8 into Eqs. 11 and 12, the following expressions result for the recovery phase of the polymer modified binder:

$$\gamma_{r1}(t) = \tau_0\Big(0.226 \cdot \left[t^{0.589} - (t-t_1)^{0.589}\right] + 2.06 \times 10^{-7} \cdot \tau_0^{3.04} \cdot \left[t^{2.04} - (t-t_1)^{2.04}\right]\Big) \tag{13}$$

$$\gamma_{r2}(t) = \tau_0\Big(0.226 \cdot \left[t^{0.589} - (t-t_1)^{0.589}\right] + 2.06 \times 10^{-7} \cdot \tau_0^{3.04} \cdot t^{2.04}\Big) \tag{14}$$

The strains predicted by Eqs. 13 and 14 were compared with the testing results for the recovery phase, and the results were not satisfactory. Figure 11 shows the testing results for 10 s of loading time and two stress levels (0.1 and 10 kPa) for the polymer modified binder. Fit1 and Fit2 correspond to the fittings using Eqs. 13 and 14, respectively. For 0.1 kPa, both fittings agree reasonably well with the recovery of the material, for the window of time considered. However, for 10 kPa, the modified superposition principle predicts an increase in the strain, even when no load was being applied.

As mentioned before, Eqs. 8 and 10 do not comply with the fading memory hypothesis. Because of the nonlinear term in both equations (the second term), there is an increase in the slope of the $J(t)$ curve for long loading times, with a stronger effect for higher stresses, which explains the unsatisfactory results obtained.

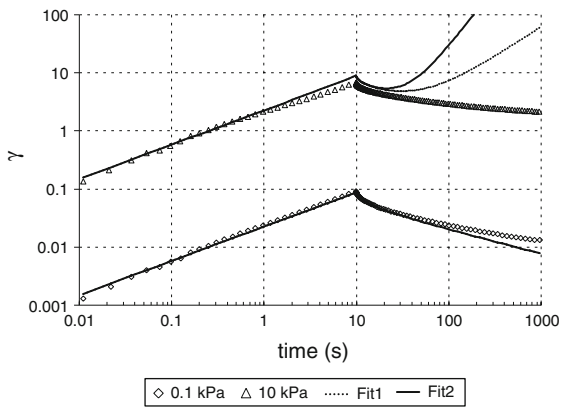

Fig. 11 Modeling of recovery phase using modified superposition principle, polymer modified binder

A similar analysis was conducted for the unmodified binder, and the results were also unsatisfactory. The complete results are not presented here because of space restrictions, but they can be looked at in the original work [9].

5.2 Modeling of the permanent strain

Since the prediction of the recovery phase by means of the modified superposition principle did not work for the selected materials, a different approach was taken in which the total strain was separated into permanent and recoverable strains, as shown in Fig. 1 and Eq. 4. In order to find the functions γ_p and γ_r, the binders needed to be tested at different stress levels and different loading times. The binder testing program described previously considered, for each binder, five stress levels and four loading times. For each testing condition, the total strain γ at the end of the loading phase was recorded. Then, after enough recovery was allowed in the material, γ_p was directly measured. Finally γ_r was calculated by subtracting γ_p from γ. It should be noted that the permanent strain and recoverable strain functions are obtained as a function of the loading time applied, but they have physical meaning only when the load is removed.

Tables 2 and 3 show the measured values of γ and γ_p for the polymer modified binder, at all testing conditions. For loading levels of 20 and 30 kPa, the test was stopped before 1,000 s of loading because the samples lost deformation resistance (free spinning) after 440 and 580 s, respectively. For this reason, and in order to obtain more data for longer times and high stresses, two extra tests were conducted using 300 s of loading at 20 and 30 kPa.

Tables 2 and 3 show that for short loading times and low stresses, γ_p is small compared to γ. For high stresses and longer loading times, however, the γ_p and γ values are of similar magnitude, becoming almost equal for the very high stresses and loading times. Table 4 shows the ratio between γ_p and γ for all testing conditions. As observed, for longer loading times and high stresses, practically all the deformation becomes permanent as the ratio reaches 100%. This means that the recoverable strain γ_r, which is calculated by the difference between γ and γ_p, becomes insignificant at high stresses and long times.

In order to select the best model to use for the permanent strain γ_p, the data were plotted in a log–log scale in Fig. 12. The chart shows linear relationship between γ_p and time for shorter times and low stresses. For higher stresses, the slope of the relationship increases. This means that the nonlinear power law can also be applied to the permanent deformation, so the model selected for γ_p was of the same form as the model used for the total strain γ: a nonlinear power law model with two arguments, one linear and one nonlinear. The behavior at higher stresses and longer times is dominated by the second argument of the model, the nonlinear part. As

Table 2 Total shear strain for different loading times, polymer modified binder

Loading time t_1 (s)	γ				
	0.1 kPa	1 kPa	10 kPa	20 kPa	30 kPa
1	0.0249	0.2469	2.204	4.800	6.425
10	0.0916	0.9306	6.929	15.96	38.55
100	0.365	3.346	37.18	535.4	2413
1000	1.721	14.55	2802	2969[a]	12570[a]

[a] Value measured at 300 s

Table 3 Permanent shear strain for different loading times, polymer modified binder

Loading time t_1 (s)	γ_p				
	0.1 kPa	1 kPa	10 kPa	20 kPa	30 kPa
1	0.0007	0.0171	0.2300	1.398	1.592
10	0.0099	0.1468	1.848	9.26	32.60
100	0.1210	1.265	29.36	532.3	2412
1000	1.080	10.50	2800	2968[a]	12560[a]

[a] Value measured at 300 s

Table 4 Ratio of total strain to permanent strain, polymer modified binder

Loading time t_1 (s)	γ_p/γ				
	0.1 kPa (%)	1 kPa (%)	10 kPa (%)	20 kPa (%)	30 kPa (%)
1	2.9	6.9	10.4	29.1	24.8
10	10.8	15.8	26.7	58.0	84.6
100	33.5	37.8	78.9	99.4	99.9
1000	62.7	72.2	99.9	99.9	100.0

discussed previously, the γ_p values approximate the γ values for high stresses and long times. For this reason, the second argument of the γ_p model was selected to be equal to the second argument obtained in the model for γ. Considering this, the γ_p data were fitted satisfactorily, with an R^2 value of 0.877. Figure 12 shows the results of the fitting with solid line. The fitting equation and parameters are:

$$\gamma_p(t,\tau) = 2.06 \times 10^{-2} \cdot t^{0.890} \cdot \tau + 2.06 \times 10^{-7} \cdot t^{2.04} \cdot \tau^{4.04} \quad (15)$$

The recoverable strain γ_r can be calculated by subtracting γ_p (Eq. 14) from γ (Eq. 7):

$$\gamma_r(t,\tau) = \tau \cdot (0.226 \cdot t^{0.589} - 2.06 \times 10^{-2} \cdot t^{0.890}) \quad (16)$$

It should be noted that the γ_r function becomes negative for times longer than 2,857 s, which does not make physical sense. However, because of the fact that for longer times the recoverable strain is insignificant compared to the permanent strain, the predictions of the model still work satisfactorily for times longer than 2,857 s, as it will be shown later in this section. The corresponding compliances for the

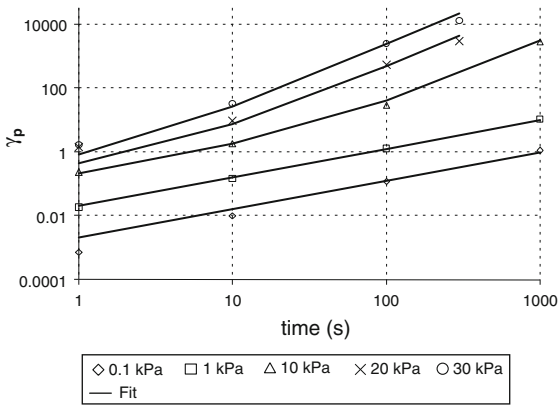

Fig. 12 Permanent strain versus loading time, measured data and fitting results, polymer modified binder

permanent strain and recoverable strains can be obtained by dividing Eqs. 15 and 16 by the shear stress:

$$J_p(t,\tau) = 2.06 \times 10^{-2} \cdot t^{0.890} + 2.06 \times 10^{-7} \cdot t^{2.04} \cdot \tau^{3.04} \,(1/\text{kPa}) \quad (17)$$

$$J_r(t) = 0.226 \cdot t^{0.589} - 2.06 \times 10^{-2} \cdot t^{0.890} \quad (1/\text{kPa}) \quad (18)$$

It should be noted that the resulting J_r is a linear viscoelastic function, according to Eq. 18, since it does not depend on the stress level. The resulting models for the creep compliances are plotted in Fig. 13 for the highest and the lowest stress levels and for the time range considered. For 30 kPa, the plot shows only until 300 s, because the sample failed (continuous deformation with no load) after this time. As with the original data, the difference between J and J_p is significant for short times and small stresses, but both functions tend to reach the same magnitude for longer times. The figure also shows the recoverable compliance J_r, whose magnitude is similar to J for shorter times, but becomes insignificant for higher stresses and longer times. The J_r curve is the same for all stresses because the J_r function does not have a stress variable, as it was shown in Eq. 18.

As with the polymer modified binder, the total strain γ and permanent strain γ_p were obtained for each testing condition for the unmodified binder. The nonlinear power law model with first argument linear, and the same second argument used in the total strain γ model, showed good agreement with the γ_p data (R^2 value of 0.953). The fitting equation and parameters are:

$$\gamma_p(t,\tau) = 4.90 \times 10^{-2} \cdot t^{0.877} \cdot \tau + 3.37 \times 10^{-3} \cdot t^{1.34} \cdot \tau^{1.25} \quad (19)$$

The recoverable strain γ_r can be then calculated by subtracting γ_p (Eq. 19) from γ (Eq. 9):

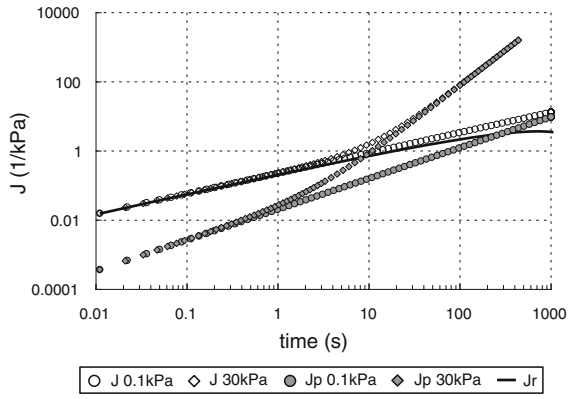

Fig. 13 Creep compliance, permanent compliance and recoverable compliance from fitted models, polymer modified binder

$$\gamma_r(t,\tau) = \tau \cdot (7.11 \times 10^{-2} \cdot t^{0.807} - 4.90 \times 10^{-2} \cdot t^{0.877}) \quad (20)$$

The function γ_r for the unmodified binder becomes negative for times longer than 203 s, which does not make physical sense. However, as explained previously, the recoverable strain for longer times is insignificant compared to the permanent strain. For this reason, the predictions from the model are still satisfactory for times longer than 203 s, as it will be demonstrated later in this section. The corresponding compliances for the permanent strain and recoverable strains can be obtained by dividing Eqs. 19 and 20 by the shear stress:

$$J_p(t,\tau) = 4.90 \times 10^{-2} \cdot t^{0.877} + 3.37 \times 10^{-3} \cdot t^{1.34} \cdot \tau^{0.25} \quad (1/\text{kPa}) \quad (21)$$

$$J_r(t) = 7.11 \times 10^{-2} \cdot t^{0.807} - 4.90 \times 10^{-2} \cdot t^{0.877} \quad (1/\text{kPa}) \quad (22)$$

The J_r resulting from the model is a linear viscoelastic function, as shown in Eq. 22. The detailed calculations and results for the unmodified binder can be found in the original work [9].

5.3 Nonlinear constitutive relationships obtained by separating permanent and recoverable strains

Once permanent and recoverable strains are separated, the total strain γ for a constant stress load τ_0 can be expressed as:

$$\gamma(t,\tau_0) = \tau_0 \cdot J_p(t,\tau_0) + \tau_0 \cdot J_r(t) \quad (23)$$

For an arbitrary load history, however, a nonlinear constitutive relationship has to be obtained. The permanent deformation γ_p is analogous to viscous deformation. For a viscous fluid, the strain due to an arbitrary stress history (starting at 0) is given by:

$$\gamma_p(t) = \int_0^t \frac{\partial \gamma_p(\xi,\tau(\xi))}{\partial \xi} d\xi = \int_0^t \dot{\gamma}_p(\xi) d\xi \quad (24)$$

where ξ is the time integration variable, and $\tau(\xi)$ is an arbitrary stress history respect to time. The time t in Eq. 24 is referenced to the start time of the stress history, defined as zero. The time t can be interpreted as $t - \xi$ with t now as running time and ξ as the start time of the stress history. The strain rate $\dot{\gamma}_p(\xi)$ can be obtained by differentiating Eq. 15 (for the polymer modified binder) or Eq. 19 (for the unmodified binder) with respect to time and then substituting the time variable t for the integration variable ξ.

The recoverable deformation γ_r, on the other hand, has the behavior of a linear viscoelastic solid for both asphalt binders, as shown by Eqs. 18 and 22. Then, the constitutive relationship for γ_r can be obtained by the Boltzmann superposition principle.

$$\gamma_r(t) = \int_0^t J_r(t-\xi) \frac{d\tau(\xi)}{d\xi} d\xi \quad (25)$$

where J_r is given by Eqs. 18 and 22 for the polymer modified binder or unmodified binder, respectively. The total strain for an arbitrary stress history can then be expressed as:

$$\gamma(t) = \int_0^t \dot{\gamma}_p(\xi) d\xi + \int_0^t J_r(t-\xi) \frac{d\tau(\xi)}{d\xi} d\xi; \quad (26)$$

5.3.1 Polymer modified binder

By differentiating Eq. 15 with respect to time, the following expression is obtained for the strain rate $\dot{\gamma}_p(t)$ of the polymer modified binder.

$$\dot{\gamma}_p(t) = 1.83 \times 10^{-2} \cdot t^{-0.110} \cdot \tau + 4.20 \times 10^{-7} \cdot t^{1.04} \cdot \tau^{4.04} + \left(2.06 \times 10^{-2} \cdot t^{0.890} + 8.32 \times 10^{-7} \cdot t^{2.04} \cdot \tau^{3.04}\right) \cdot \frac{d\tau(t)}{dt} \quad (1/s) \tag{27}$$

By inserting Eqs. 18 and 27 into Eq. 26, and substituting to the time integration variable ξ, the following nonlinear constitutive relationship is obtained for the polymer modified binder:

$$\gamma(t) = \int_0^t \left\{1.83 \times 10^{-2} \cdot \xi^{-0.110} \cdot \tau + 4.20 \times 10^{-7} \cdot \xi^{1.04} \cdot \tau^{4.04} + \left(2.06 \times 10^{-2} \cdot \xi^{0.890} + 8.32 \times 10^{-7} \cdot \xi^{2.04} \cdot \tau^{3.04}\right) \cdot \frac{d\tau(\xi)}{d\tau}\right\} d\xi + \int_0^t \left\{0.226 \cdot (t-\xi)^{0.589} - 2.06 \times 10^{-2} \cdot (t-\xi)^{0.890}\right\} \frac{d\tau(\xi)}{d\xi} d\xi \quad (1/s) \tag{28}$$

5.3.2 *Unmodified binder*

The strain rate $\dot{\gamma}_p(t)$ for the unmodified binder is obtained by differentiating Eq. 19 with respect to time.

$$\dot{\gamma}_p(t) = 4.30 \times 10^{-2} \cdot t^{-0.123} \cdot \tau + 4.52 \times 10^{-3} \cdot t^{0.34} \cdot \tau^{1.25} + \left(4.90 \times 10^{-2} \cdot t^{0.877} + 4.21 \times 10^{-3} \cdot t^{1.34} \cdot \tau^{0.25}\right) \cdot \left(\frac{d\tau(t)}{dt}\right) \tag{29}$$

The nonlinear constitutive relationship for the unmodified binder is obtained by inserting Eqs. 22 and 29 into Eq. 26 and substituting to the time integration variable ξ.

$$\gamma(t) = \int_0^t \left\{4.30 \times 10^{-2} \cdot \xi^{-0.123} \cdot \tau + 4.52 \times 10^{-3} \cdot \xi^{0.34} \cdot \tau^{1.25} + \left(4.90 \times 10^{-2} \cdot \xi^{0.877} + 4.21 \times 10^{-3} \cdot \xi^{1.34} \cdot \tau^{0.25}\right) \cdot \left(\frac{d\tau(\xi)}{d\xi}\right)\right\} d\xi + \int_0^t \left\{7.11 \times 10^{-2} \cdot (t-\xi)^{0.807} - 4.90 \times 10^{-2} \cdot (t-\xi)^{0.877}\right\} \frac{d\tau(\xi)}{d\xi} d\xi \tag{30}$$

6 Prediction of testing results using the obtained nonlinear constitutive relationships

The binder testing was performed using creep and recovery loading. This loading pattern can be expressed mathematically using the Heaviside step function:

$$\tau(t) = \tau_0 H(t) - \tau_0 H(t - t_1) \tag{31}$$

where τ_0 represents the constant creep stress, and t_1 is the loading time. By substituting Eq. 31 into Eq. 26, the following expression is obtained for the creep and recovery:

$$\gamma(t) = \begin{cases} \tau_0 \cdot \left(J_p(t,\tau_0) + J_r(t)\right), & t \le t_1 \\ \tau_0 \cdot J_p(t_1,\tau_0) + \tau_0 \cdot J_r(t) - \tau_0 \cdot J_r(t-t_1), & t_1 < t \end{cases} \tag{32}$$

where $t \le t_1$ corresponds to the loading phase, and $t > t_1$ is the recovery phase. The functions J_p and J_r are the ones described in Eqs. 17 and 18 for the polymer modified binder, and in Eqs. 21 and 22 for the unmodified binder.

The results of the prediction for the polymer modified binder are presented in Figs. 14 and 15, for 10 and 100 s loading time, respectively. The prediction of the recovery phase agrees reasonably well with the testing data. The creep fitting portion also agrees well, as it was already verified previously. For the unmodified binder, the results of the prediction are presented in Figs. 16 and 17, for 10 and 100 s loading time, respectively. The predictions for this material also agree well with the testing data.

7 Validation of nonlinear constitutive relationships with MSCR test results

The nonlinear constitutive relationships should be able to describe the behavior for any kind of loading patterns. In order to verify this, testing results using MSCR test were compared with the predictions from the model. MSCR is a test currently used for evaluating the nonlinearity of asphalt binders, and it was described previously. The loading pattern consisted of 10 cycles of creep and recovery with 0.1 kPa shear stress followed immediately by 10 cycles of

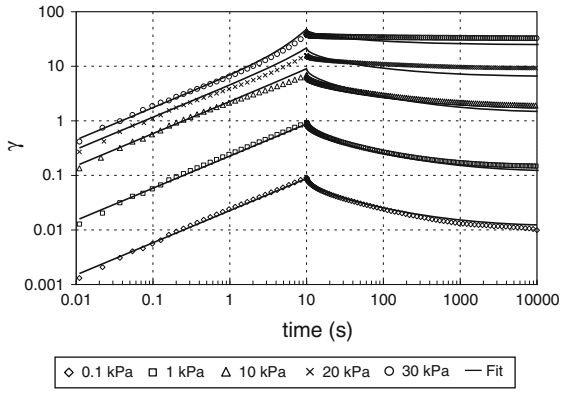

Fig. 14 Testing data and fitting curves, 10 s loading time, polymer modified binder

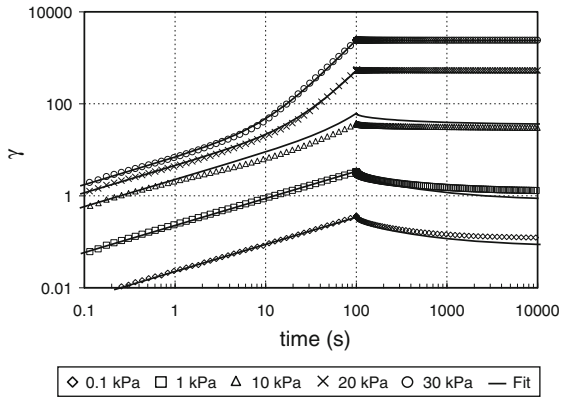

Fig. 15 Testing data and fitting curves, 100 s loading time, polymer modified binder

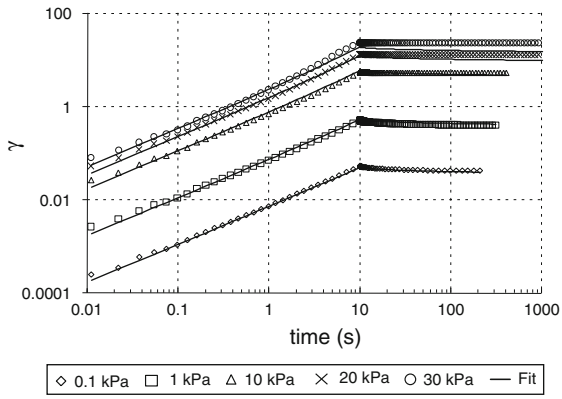

Fig. 16 Testing data and fitting curves, 10 s loading time, unmodified binder

creep and recovery at 3.2 kPa shear stress. Each cycle had 1 s of creep and 9 s of recovery, for a total of 200 s test duration. Using the Heaviside step function H, the MSCR loading pattern can be described as:

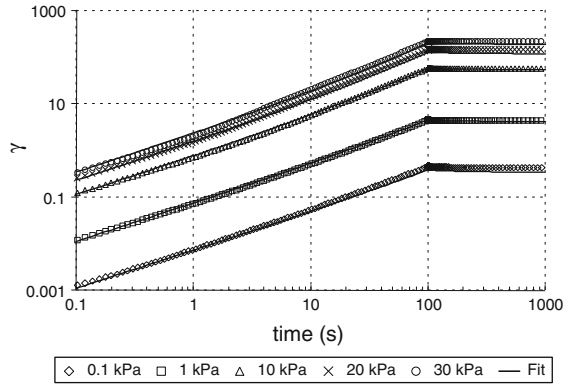

Fig. 17 Testing data and fitting curves, 100 s loading time, unmodified binder

$$\tau(t) = \tau_1 \sum_{i=1}^{10} \{H(t - t_{2i-2}) - H(t - t_{2i-2})\}. + \tau_2 \sum_{i=11}^{20} \{H(t - t_{2i-2}) - H(t - t_{2i-1})\} \tag{33}$$

where $\tau_1 = 0.1$ kPa, $\tau_2 = 3.2$ kPa, $t_0 = 0$ s, $t_1 = 1$ s, $t_2 = 10$ s, $t_3 = 11$ s, …,$t_{18} = 90$ s, $t_{19} = 91$ s, $t_{20} = 100$ s, $t_{21} = 101$ s, $t_{22} = 110$ s, $t_{23} = 111$ s, …, $t_{38} = 190$ s, $t_{39} = 191$ s.

By substituting Eq. 33 into Eq. 26 and performing the integration, the following expressions are obtained for the strain response γ(t) of the MSCR test in the first four intervals.

For $0 < t \leq 1$ s:

$$\gamma(t) = \tau_1 \cdot \{J_p(t, \tau_1) + J_r(t)\} \tag{34}$$

For $1 < t \leq 10$ s:

$$\gamma(t) = \tau_1 \cdot \{J_p(1, \tau_1) + J_r(t) - J_r(t-1)\} \tag{35}$$

For $10 < t \leq 11$ s:

$$\gamma(t) = \tau_1 \cdot \{J_p(1, \tau_1) + J_r(t) - J_r(t-1) + J_p(t-10, \tau_1) + J_r(t-10)\} \tag{36}$$

For $11 < t \leq 20$ s:

$$\gamma(t) = \tau_1 \sum_{i=1}^{2} \{J_p(t_{2i-1} - t_{2i-2}, \tau_1), + J_r(t - t_{2i-2}) - J_r(t - t_{2i-1})\} \tag{37}$$

The expressions for γ(t) in the remaining time intervals follow the same pattern. Using the corresponding J_p and J_r functions for each material, the

strain predictions were programmed in an Excel spreadsheet.

Using the DSR with cone and plate geometry, one sample of each asphalt binder was run with the MSCR loading pattern at 46°C. The comparison of results of the testing data and model predictions are shown in Figs. 18 and 19 for the polymer modified binder and unmodified binder, respectively. The results presented in a logarithmic scale allow observing the general fitting during the all testing sequence. It can be observed that the predictions from the models have good agreement with the testing data for both materials.

A more detailed comparison of the results can be achieved with cross plots between the measured and predicted values, as presented in Figs. 20 and 21. For the polymer modified binder, the model predictions follow the same trend that the measured data, but there is an under prediction of the results. The maximum error was observed towards the end of the test, reaching a value of 20.5% difference respect to the measured values. For the unmodified binder, the model also follows the trend of the data, but it over predicts the measured values. The maximum difference measured towards the end of the test was 16.8%.

The prediction errors were in one direction for the first material (underprediction) and in the opposite direction for the second material, but with very similar error magnitudes. It is reasonable to conclude then that the errors are due to testing variability and not to model bias. This conclusion needs to be confirmed with further testing including more materials.

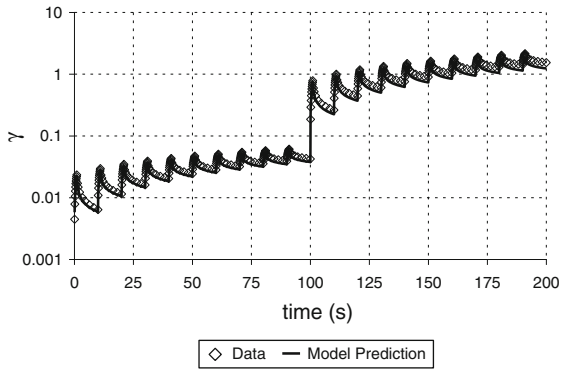

Fig. 18 MSCR test results and fitting, polymer modified binder

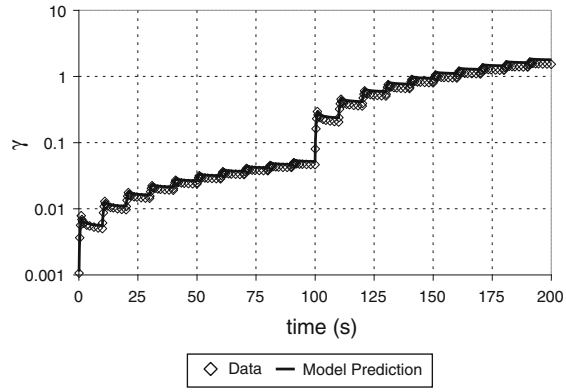

Fig. 19 MSCR test results and fitting, unmodified binder

8 Conclusions

- The creep behavior of the two asphalt binders tested showed a nonlinear power law behavior.
- A nonlinear power law model with two arguments, one linear respect to the stress, and one nonlinear, was successful in fitting the creep response of the binders for all stress levels.
- Since the creep compliance functions selected did not comply with the fading memory hypothesis, the modified superposition principle was unable to predict the recovery response of the binders for the time range and stress range considered in the test.
- A nonlinear constitutive relationship composed of a viscous nonlinear part plus a linear viscoelastic part predicted successfully the testing results in creep and recovery.

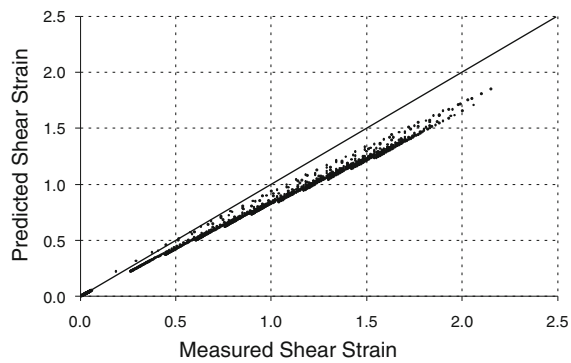

Fig. 20 Cross plot of measured strain versus predicted strain, polymer modified binder

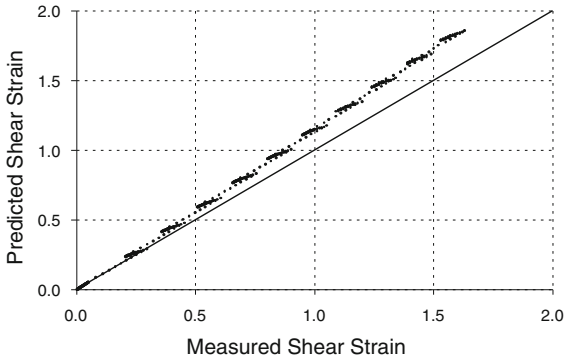

Fig. 21 Cross plot of measured strain versus predicted strain, unmodified binder

- The nonlinear constitutive relations were able to predict the response of the binders using the MSCR protocol. The maximum differences between the measured and predicted values were observed towards the end of the test, reaching values up to 20%. The differences can be reasonably assumed to be testing variability.
- Some of the limitations of the present work are: (a) the model developed is valid for the time range considered in the testing. Extrapolations outside those ranges are not necessarily accurate; (b) deformations were measured in one dimension only; (c) stress reversal was not studied in this work and (d) further work is needed to include temperature effects in the characterization.

References

1. Anderson DA, Christensen DW, Bahia HU (1991) Physical properties of asphalt cement and the development of performance related specifications. J Assoc Asph Paving Technol 60:437–475
2. Anderson D, Le Hir YM, Marasteanu M, Planche JP, Martin D, Gauthier G (2001) Evaluation of fatigue criteria for asphalt binders. Transp Res Rec J Transp Res Board 1766:48–56
3. Bahia HU, Hanson DI, Zeng M, Zhai H, Khatri MA, Anderson RM (2001) Characterization of modified asphalt binders in superpave mix design. National Cooperative Highway Research Program, Report NCHRP 459. National Academy Press, Washington
4. Boltzmann L (1874) "Zur Theorie der Elastischen Nachwirkungen", Sitzungsber. Kaiserlich Akad Wissen Math. Naturwissen 70:275–306
5. Bonifasi-Lista C, Lake SP, Small MS, Weiss JA (2005) Viscoelastic properties of the human medial collateral ligament under longitudinal, transverse, and shear loading. J Orthop Res 23:67–76
6. Buchdahl R, Nielsen L (1951) The application of Nutting's equation to the viscoelastic behavior of certain polymeric systems. J Appl Phys 22(11):1344–1349
7. Chen JS, Kuo PH, Lin PS, Huang CC, Lin KY (2008) Experimental and theoretical characterization of the engineering behavior of bitumen mixed with mineral filler. Mater Struct 41(6):1015–1024
8. D'Angelo J, Kluttz R, Dongre R, Stephens K, Zanzotto L (2007). Revision of the superpave high temperature binder specification: the multiple stress creep recovery test. J Assoc Asph Paving Technol 76:123–157
9. Delgadillo R (2008) Nonlinearity of asphalt binders and the relationship with asphalt mixture permanent deformation. PhD Thesis, The University of Wisconsin, Madison
10. Delgadillo R, Bahia HU (2010) The relationship between nonlinearity of asphalt binders and asphalt mixture permanent deformation. Road Mater Pavement Des 11:653–680
11. Delgadillo R, Cho DW, Bahia HU (2006) Nonlinearity of repeated creep and recovery binder test and the relationship with mixture permanent deformation. Transp Res Rec J Transp Res Board, No. 1962. TRB, National Research Council, Washington, pp. 3–11
12. Delgadillo R, Nam K, Bahia HU (2006) Why do we need to change G*/sinδ and how? Road Mater Pavement Des 7(1):7–27. Hermes Science Publications
13. Di Benedetto H, Neifar M, Sauzeat C, Olard F (2007) Three-dimensional thermo-viscoplastic behavior of bituminous materials: the DBN model. Int J Road Mater Pavement Des 8(2):285–316
14. Findley WN, Davis FA, Lai JS, Onaran K (1989) Creep and relaxation of nonlinear viscoelastic materials. Dover Publications, New York
15. Huang Y (1993) Pavement analysis and design. Prentice Hall, Englewood Cliffs
16. Isacsson U, Lu X (1995) Testing and appraisal of polymer modified road bitumens—state of the art. Mater Struct 28(3):139–159
17. Kose S (2001) Development of a virtual test procedure for asphalt concrete. PhD Thesis, University of Wisconsin, Madison
18. Kose S, Guler M, Bahia H, Masad E (2000) Distribution of strains within binders in HMA using imaging and finite element techniques. Transp Res Rec J Transp Res Board 1728:21–27. Washington DC
19. Lai J, Anderson D (1973) Irrecoverable and recoverable nonlinear viscoelastic properties of asphalt concrete. Highway research records. J Transp Res Board 468:73–88
20. Lakes RS (2009) Viscoelastic materials. Cambridge University Press, New York
21. Lakes RS, Kose S, Bahia H (2002) Analysis of high volume fraction irregular particulate damping composites. ASME J Eng Mater Technol 124:174–178
22. Lockett FJ (1965) Creep and stress-relaxation experiments for nonlinear materials. Int J Eng Sci 3:59–75. Pergamon Press
23. Neifar M, Di Benedetto H (2001) Thermo-viscoplastic law for bituminous mixes. Int J Road Mater Pavement Des 2(1):71–95

24. Nutting P (1921) A study of elastic viscous deformation. Proc Am Soc Test Mater 21:1162–1171
25. Pipkin A, Rogers TG (1968) A non-linear representation for viscoelastic behavior. J Mech Phys Solids 16:59–72
26. Reinke G, Glidden S, Engber S, Herlitzka D (2006) Rheological properties of polymer modified binders and mixtures related to mixture resistance to permanent deformation. Proceedings of the fifty first annual conference of the Canadian Technical Asphalt Association (CTAA), Charlottetown, Prince Edward Island, Nov 5–8, pp 57–85
27. Schapery RA (1997) Nonlinear viscoelastic and viscoplastic constitutive equations based on thermodynamics. Mech Time-Depend Mater 1:209–240
28. Schapery RA (1999) Nonlinear viscoelastic and viscoplastic constitutive equations with growing damage. Int J Fract 97(1):33–66
29. Sternstein SS (1973) Private communication
30. Synergy (2002) KaleidaGraph Software: Release 3.5
31. Ward IM, Wolfe JM (1966) The non-linear mechanical behavior of polypropylene fibers under complex loading. J Mech Phys Solids 14:131–140